Remote Sens. **2012**, *4*, 135-159; doi:10.3390/rs4010135

OPEN ACCESS

Remote Sensing

ISSN 2072-4292

www.mdpi.com/journal/remotesensing

Article

Modeling Forest Structural Parameters in the Mediterranean Pines of Central Spain using QuickBird-2 Imagery and Classification and Regression Tree Analysis (CART)

Cristina Gómez [1,*], Michael A. Wulder [2], Fernando Montes [3] and José A. Delgado [1]

[1] Sustainable Forest Management Research Institute, Universidad de Valladolid, E-34004 Palencia, Spain; E-Mail: joseant@latuv.uva.es

[2] Pacific Forestry Centre, Canadian Forest Service, Natural Resources Canada, Victoria, BC V8Z 1M5, Canada; E-Mail: mike.wulder@nrcan.gc.ca

[3] Departamento de Sistemas y Recursos Forestales, CIFOR-INIA, Ctra. de La Coruña km 7.5, E-28040 Madrid, Spain; E-Mail: fmontes@inia.es

* Author to whom correspondence should be addressed; E-Mail: c.gomez@abdn.ac.uk; Tel.: +1-281-712-5614.

Received: 25 October 2011; in revised form: 4 January 2012 / Accepted: 4 January 2012 / Published: 10 January 2012

Abstract: Forest structural parameters such as quadratic mean diameter, basal area, and number of trees per unit area are important for the assessment of wood volume and biomass and represent key forest inventory attributes. Forest inventory information is required to support sustainable management, carbon accounting, and policy development activities. Digital image processing of remotely sensed imagery is increasingly utilized to assist traditional, more manual, methods in the estimation of forest structural attributes over extensive areas, also enabling evaluation of change over time. Empirical attribute estimation with remotely sensed data is frequently employed, yet with known limitations, especially over complex environments such as Mediterranean forests. In this study, the capacity of high spatial resolution (HSR) imagery and related techniques to model structural parameters at the stand level (n = 490) in Mediterranean pines in Central Spain is tested using data from the commercial satellite QuickBird-2. Spectral and spatial information derived from multispectral and panchromatic imagery (2.4 m and 0.68 m sided pixels, respectively) served to model structural parameters. *Classification and Regression Tree Analysis* (CART) was selected for the modeling of attributes. Accurate models were produced of quadratic mean diameter (QMD) (R^2 = 0.8; RMSE = 0.13 m) with an average error of 17% while basal area (BA) models produced an average error of 22% (RMSE = 5.79 m^2/ha).

When the measured number of trees per unit area (N) was categorized, as per frequent forest management practices, CART models correctly classified 70% of the stands, with all other stands classified in an adjacent class. The accuracy of the attributes estimated here is expected to be better when canopy cover is more open and attribute values are at the lower end of the range present, as related in the pattern of the residuals found in this study. Our findings indicate that attributes derived from HSR imagery captured from space-borne platforms have capacity to inform on local structural parameters of Mediterranean pines. The nascent program for annual national coverages of HSR imagery over Spain offers unique opportunities for forest structural attribute estimation; whereby, depletions can be readily captured and successive annual collections of data can support or enable refinement of attributes. Further, HSR imagery and associated attribute estimation techniques can be used in conjunction, not necessarily in competition to, more traditional forest inventory with synergies available through provision of data within an inventory cycle and the capture of forest disturbance or depletions.

Keywords: forest structure; high spatial resolution; image segmentation; CART; monitoring

1. Introduction

Sustainable management of Mediterranean pine forests requires detailed and up-to-date information regarding structural parameters [1]. Wood volume and biomass content in forest stands, calculated with structural indicators such as mean height and quadratic mean diameter, are basic data for administration of resources. Moreover, increasingly important and emerging environmental concerns related to habitat protection, carbon accounting, and biodiversity, make reliable knowledge of forest resources a requirement for national and international reporting [2].

In Spain, as in many other countries, accurate information of structural parameters is usually obtained via direct measurements by crews on the ground of systematically sampled field inventories, based upon a network of plots located on a regular grid [3] that is also subject to prior stratification. Field surveys are often costly and typically not spatially exhaustive. Field surveys are also often collected over a given re-measurement period, which can preclude adequate updating of information for periodic reports, and are of questionable validity over dynamic or non-merchantable forests. Despite these concerns, ground based inventories provide reliable and detailed information for development of models such as yield tables per species and given location. It is the difficulties in portraying these plot based measures spatially that for many applications limit the utility of this information to address more broad forest monitoring and reporting objectives [4], especially in heterogeneous forests.

Satellite imagery has been shown to support forest inventories of extensive areas by providing timely observation, increasing the accuracy of area estimates, producing wall-to-wall thematic maps, and providing inventory estimates with acceptable bias and precision [5]. The spatially detailed information provided by high spatial resolution (HSR) imagery makes it an appropriate data source to

aid in accurate estimation of structural parameters, and following suitable methods facilitates the characterization of subtle changes in forest structure through time [6].

The goal of this research is to explore the potential of HSR imagery to characterize forest structure in Mediterranean pines in the Central Range of Spain. Motivated by this purpose we examine the capacity of QuickBird-2 imagery to model the quadratic mean diameter, basal area, and number of trees per unit area at the stand level (as direct estimators of volume and biomass). Our specific objectives are:

- To model the relation between structural parameters (quadratic mean diameter, basal area, and number of stems per hectare) measured via field sampling and a set of spectral and spatial variables derived from HSR multispectral and panchromatic imagery.
- To test and verify the ability of Classification and Regression Trees (CART) as the statistical technique for modeling structural parameters.
- To identify the image derived variables with the greatest informative capacity in the modeling of structural parameters, assessing in particular the inclusion of image textural metrics in the models.

2. Background

Space-borne optical remote sensing is a reliable source of information for assessment of forest characteristics over wide areas [7]. The synoptic view and the regular acquisition cycle of image data, combined with the burgeoning selection of techniques available for attribute estimation, make remotely sensed data an appropriate and valuable source of data for assessment of forest condition and detection of change—offering information to augment costly and time consuming field campaigns for inventory update and re-measurement [8].

2.1. High Spatial Resolution (HSR) Imagery

Spatial resolution is an important consideration when using remote sensing for forest characterization [9]. Currently the spatial resolution of systems frequently used for vegetation characterization range from coarse (e.g., 1 km of the Advanced Very High Resolution Radiometer) to very high (e.g., 0.4 m of the GeoEye-1 sensor). The adequacy of remotely sensed data for a specific purpose (e.g., attribute level: tree, stand, landscape, region) is conditioned by its spatial resolution, which is also inversely related to the extent covered by the image [10], also known as the image footprint.

Medium spatial resolution data with pixels sized 10–100 m (e.g., Landsat Thematic Mapper (30 m), ASTER (15 m)) are appropriate for characterization of forest condition [11] and monitoring of conditions and change at the forest stand level [12]. Certainly a key to the applications and monitoring success of Landsat is the ability to capture conditions and dynamics that relate human interaction with terrestrial ecosystems. However, more detailed spatial data available since the launch of various commercial satellites (e.g., IKONOS in 1999, Orbview-3 in 2003) provide the opportunity for more precise depiction of forest parameters and are poised to reduce estimation errors of forest attributes to an acceptable level for operational applications [13]. HSR imagery facilitates, for instance, the detection of individual tree characteristics [14], providing improved estimates of forest structural

attributes [7]. Panchromatic imagery, with fine spatial resolution (< 1 m) is particularly well suited for analysis of spatial relations through image texture measures [15,16]. Texture measures enable the combination of spatial detail of panchromatic imagery with unique spectral information conferred by multispectral imagery serving to leverage complementary information [17] that can be employed separately or with a pan-sharpening approach [18,19]. Spectral measures may be understood to inform on vegetation status, type, and condition with textural measures informing on vegetation structure.

Still, the dearth of established methods for image processing and the complex interactions between sun-sensor-surface geometry and forest structural characteristics [20], particularly in complex topographies, persist in making the use of HSR data challenging [6]. HSR imagery acquired using space-borne platforms allows for data collection over remote areas, with predictable georadiometic qualities, and information content analogous to mid-scale aerial photography—commonly used for forest inventory purposes. Lidar (Light detection and ranging) technology has a demonstrated capacity to characterize forest structure [21–24] albeit with high costs persisting to limit operational, wide-area applications [25]. Although lidar, with a capacity to collect highly detailed information regarding forest attributes, shows promise as a means to collect plot-like data for training attribute estimation algorithms applied to HSR imagery.

2.2. HSR Related to Forest Structure

The research literature is replete with studies relating forest structural parameters estimated from HSR satellite data (Table 1). Frequent techniques to obtain information from HSR images include *crown isolation* [26,27], *shadow analysis* [18,28], *texture analysis* [13,29,30], and *geostatistical* approaches [31–33]. The capacity to characterize forest structural attributes typically decreases as crown closure increases [6], with an asymptotic relationship predictably emerging for vertically distributed attributes of forest structure [34].

Table 1. Studies employing satellite HSR imagery for estimation of forest structural parameters.

Study	**Attribute**	**Environment**	**Sensor**	**Statistical Analysis**	**Best Result**
		Location	**Data (spa. res., m)**	**Parameter**	
[29]	Age class	Sooke River watershed	IKONOS	ANOVA	Homogeneity in large window sizes performs better than variance
		British Columbia (Canada)	Pan (0.82)	Texture measures	
[26]	Stem density	Conifer plantation	IKONOS	Delineation	83% accuracy
		Ontario (Canada)	Pan (0.87)	Tree crown delineation	
[35]	Diameter	Lake Tanoe Basin	IKONOS	Linear regression	R = 0.67
	Crown area	California (USA)	Pan-sharpened (1)	Crown shadow	R = 0.77
	Stem density				R = 0.87
[13]	Circumference	Even aged Norway spruce forest	IKONOS-2	Linear regression	R^2 = 0.82
	Height				R^2 = 0.76
	Stand density	Hautes-Fagnes (Belgium)	Pan (0.87)	GLCM textural metrics	R^2 = 0.82
	Age				R^2 = 0.81
	Basal area				R^2 = 0.35

Table 1. *Cont.*

[36]	Maximum height	Conifers	QuickBird	Linear regression	R^2=0.66
		Sierra Nevada mountains California (USA)	MS (2)	Reflectance	
[37]	Height Age Crown closure	Mature forest in the foothills of the Rocky Mountains	IKONOS	Decision tree	Accuracy 49% Accuracy 57% Accuracy 85%
		Alberta (Canada)	MS (4) and Pan (1)	Reflectance and texture	
[28]	Biomass	Boreal spruce forest	QuickBird	Linear regression	R^2 = 0.87
		Canada	Pansharpened (0.6)	Shadow fraction	
[31]	Mean crown size	Conifer and hardwood	IKONOS	Linear regression	R^2 = 0.73 RMSE = 0.10
		North Carolina (USA)	Pan (not reported)	Variogram Image variance ratio	
[38]	Biomass	Mangrove	IKONOS	Linear regression	R^2 = 0.92
		French Guiana	NIR (4) Pan (1)	Fourier textural ordination indices	
[27]	Stand density Stand volume	Coniferous plantations in slopes	QuickBird	Modeling-allometry	R = 0.82 density R = 0.78 volume
		Shikoku Iskland (Japan)	Pan (0.61)	Reflectance	
[39]	Crown width Tree diameter Stem frequency	Tropical forest	IKONOS	Allometric equations	Crown within 3% of field measures
		Brazil	Pan (1.00)	Local extreme filter	
[18]	Volume	Open *Juniperus* forest	QuickBird	Linear regression	R^2 = 0.67 R^2 = 0.51
		Turkey	Pansharpened (0.61)	Shadow area Crown area	
[32]	Mean crown size	Pine and poplar plant.	QuickBird	Variogram	Error: 2.52-42%
		Beijing and Shanxi, (China)	Pan (0.61-0.67)	Reflectance	
[16]	Mean crown size	Hardwoods	IKONOS and QuickBird	Linear regression	R^2 = 0.60 regression CD~variance ratio (RMSE = 0.82) R^2 = 0.74 across site comparison R^2 = 0.52 across sensors
		Ohio and North Carolina (USA)	Pan (1) Pan (0.73)	Image variance ratio	
[40]	Mean stand height	Boreal forest	QuickBird	Regression tree	R^2 = 0.53 RMSE=2.84 m
		Yukon, Canada	Pan (0.68)	Reflectance	

2.3. Status in the Use of Remote Sensing for Estimation of Forest Structure in Spain

The Spanish Plan Nacional de Teledetección (PNT) is committed to acquiring complete national coverages of HSR satellite imagery annually [41] and to make data available for research at no cost. The acquisition phase started in 2008 [42], capitalizing upon archival data to backdate the database to

2005 coverage. Initial coverage consist of SPOT5-HRG XS+P (2.5 m) data, with other sensors being considered for future acquisitions [43]. Access to this data represents a unique opportunity to incorporate HSR into Spanish forest inventories as an operational and low cost data source to meet a range of information needs. The data is to be collected with a primary focus on land-use land-cover change assessment [42], but capacity to generate information for forest monitoring and reporting can also be generated.

Encouraged by a readily available source of data there has recently been an increased interest by the Spanish research community in relation to remote sensing technologies and the potential application to forest environments, in particular the characterization of forest structure. Vázquez de la Cueva [44] explored relationships between forest structural attributes at the plot level (e.g., height, basal area, and crown canopy closure) and spectral information derived from Landsat Enhanced Thematic Mapper Plus (ETM+; 30 m pixel size) imagery combined with topographic data. The study considered three types of forest in Central Spain and applied a multivariate canonical ordination method. The author found a strong influence of vegetation type on the results, with a low percentage of variance explained precluding development of robust empirical models. Pascual *et al*. [45] used lidar data and a two stage object based methodology to characterize the structure of *Pinus sylvestris* L. stands in forests of Central Spain. Five structure types were defined based on height and density parameters. The median and standard deviation of height were found to be the most valuable for definition of structure types, with the approach developed being proposed for operational application suitable for inclusion in forest inventory procedures in support of forest management plans. Merino de Miguel *et al.* [33] investigated the strength of relations between dasometric parameters and textural variables in *Pinus pinaster* Ait. stands in Central Spain. The authors used geostatistical tools (*i.e.*, variograms), calculated with orthophotography and IKONOS-2 imagery with original and degraded spatial resolutions. The authors found the strongest correlations when the variogram was calculated for spatial resolutions of 1 m and 2 m. As such, opportunities to further explore the capacity of HSR imagery to estimate a range of forest structural parameters remain.

3. Methods

Below, and in Figure 1, we summarize the approach implemented and the data utilized in this research. Forest structural attributes (QMD, BA, and N) are derived from data measured on the field through a process of geostatistical interpolation. Spectral and spatial variables from HSR imagery direct the delineation of stand-like areas for summarizing data. Statistical models linking forest parameters and imagery data are built with CART and validated with numerical and graphical tools.

3.1. Study Area and Field Data

The study focuses on pines in the Central Range of Spain (Figure 2), an area mainly dominated by *P. sylvestris* L., *P. pinaster* Ait., and *P. nigra* Arn. species. Two sites representing different forest conditions were chosen for availability of field data. *Pinar de Valsaín* (hereafter *Valsaín*) is a 7,627 ha forest of *Pinus sylvestris* L. on the North facing slopes of Sierra de Guadarrama (Segovia). It is a multifunctional forest (timber production, recreation, and protection) with an established management plan since 1889 that has evolved from a rigid to a more flexible scheme over the subsequent decades.

Management actions and recreational activities have had an impact on the forest structure [46]. *Valle de Iruelas* (hereafter *Iruelas*) is a 5,483 ha forest of *P. pinaster* Ait., *P. sylvestris* L., and *P. nigra* Arn. in Sierra de Gredos (Ávila). It is also a multifunctional forest (wood, resin, and pasture production, recreation, and wildlife habitat). Although the first management plan was approved in 1886, historical circumstances prevented its implementation. The production of resin during the twentieth century favoured old growth development and a complex history of fires has also conditioned the forest structure.

Figure 1. Schematic methodology followed in the study.

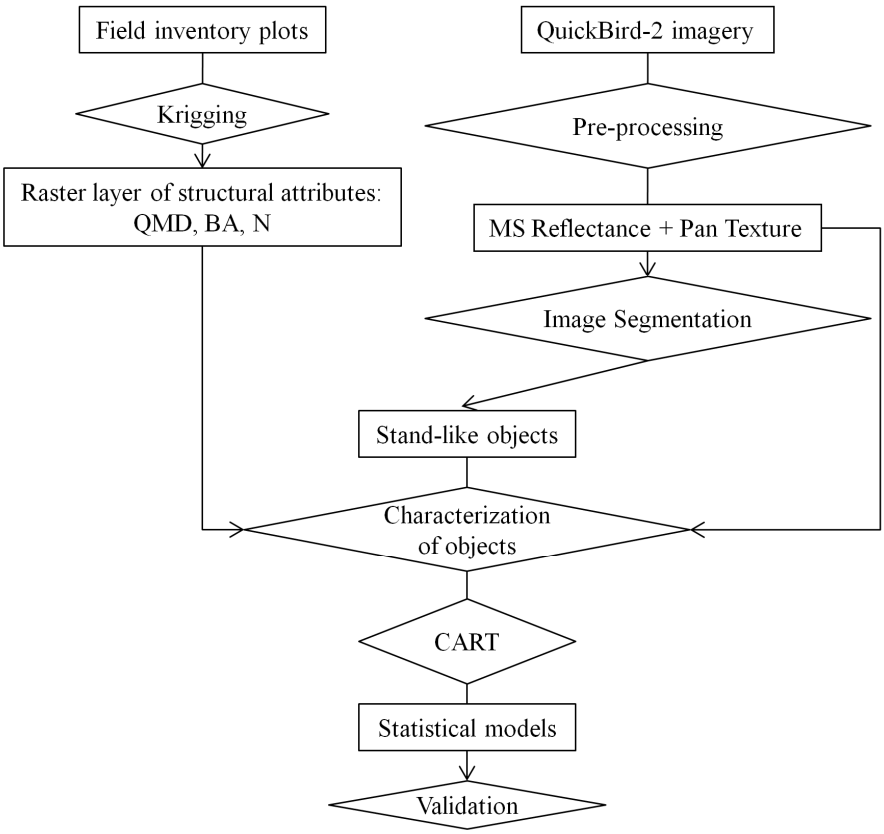

Systematic surveys based on ground sample plots are conducted periodically over the study sites measuring attributes including density, diameter at breast height (dbh), and height. For this study, data is from 2005 for *Iruelas* and 1999 for *Valsaín*, with the latter updated to 2004 conditions using a locally appropriate growth model following procedures recommended by the Spanish National Forest Inventory. The quadratic mean diameter (QMD) and basal area (BA) were calculated at each inventory plot (Equations (1–2)) where the total number of trees per unit area (N) was also available; expansion factors were used to scale values to a given area [47]. BA and QMD are adequate attributes for volume modeling at the stand level. QMD was preferred over the arithmetic mean diameter as it has a stronger correlation to stand volume [48].

$$QMD = \sqrt{\frac{\sum_i d_i^2}{N}} \tag{1}$$

$$BA = \frac{\Pi}{4} * \sum_i d_i^2 \tag{2}$$

Figure 2. Location of the study sites. Insets show QMD values as kriged from inventory plots in the treed areas of *Valle de Iruelas* and *Pinar de Valsaín*. Subset areas covered by 834 plots in *Valsaín* and 661 plots in *Iruelas* were investigated in the study.

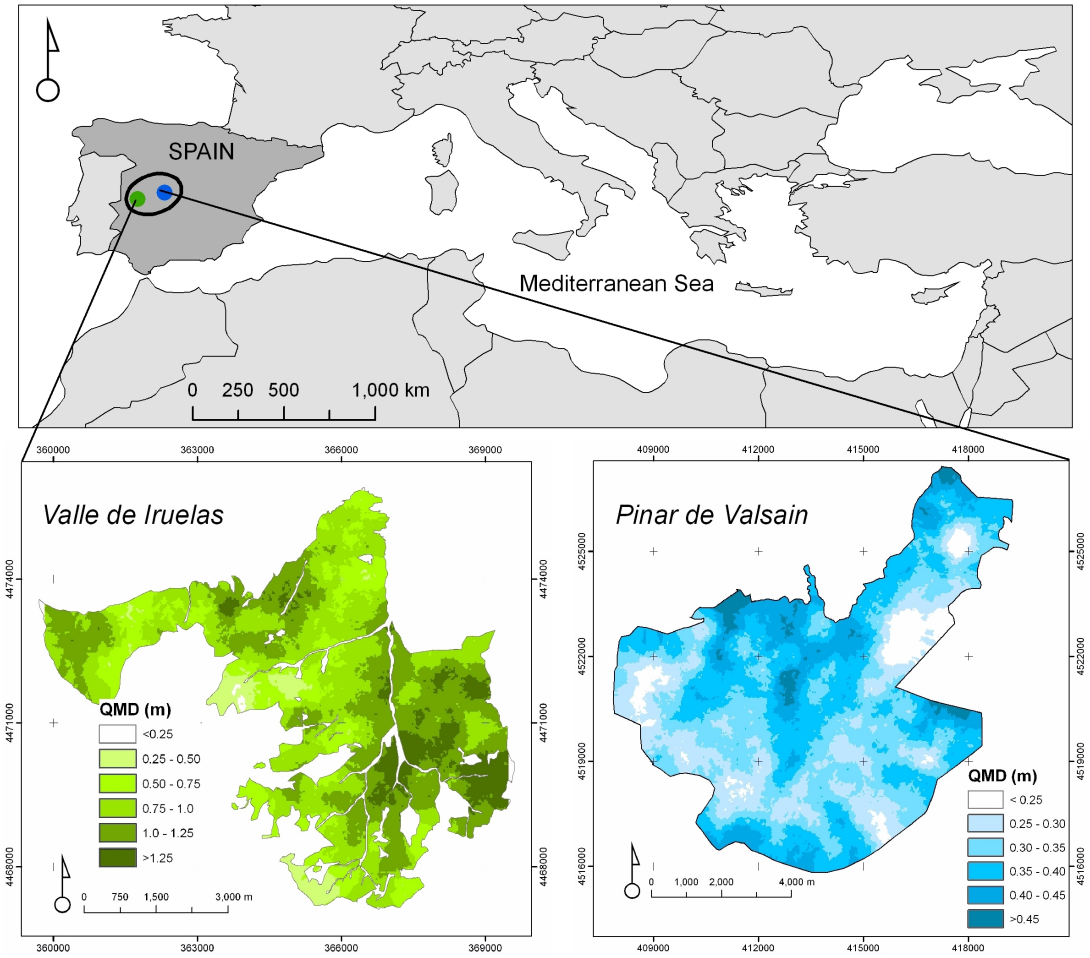

Geostatistics provides a means for extrapolation of measured values to unmeasured points and areas, and facilitates the derivation of thematic layers for integration with other data [49]. Kriging is a spatial interpolation method that yields the best possible estimation of the spatial variable of interest at every unmeasured point [50] and the error committed in the estimation is minimized and known at each point [51]. In this study we mapped the forest variables of interest (QMD, BA, and N) measured in ground plots located over grids sided 150 m in *Iruelas* and 200 m in *Valsaín* into raster layers through a process of ordinary kriging. The relative standard error (*i.e.*, the standard error of the kriged surface relative to the mean attribute value at the polygon level) was on average 15% for the QMD kriged layer and 25% for the BA and N layers, similar to the variability found for multiple plots found within the same polygon. More accurate averaging is facilitated, as sampling is complete and spatial correlation of plot values is accounted for.

3.2. HSR Imagery

QuickBird-2 is an Earth Observation satellite launched by Digital Globe in 2001, providing data in five spectral bands (Table 2). It has the capacity to be oriented and to capture images off nadir enabling

a temporal revisit of 2–6 days depending on latitude [52]. The pixel size of QuickBird-2 images is 2.4 m for the multispectral bands and 0.68 m for the panchromatic band (Table 2).

Two QuickBird-2 images, supplied in a georeferenced form by the data provider were used in this study, each covering one of the study sites (Figure 2, Table 2). Images were orthorectified with a Digital Elevation Model (DEM) derived from a contour vector map 1:10,000 (www.sitcyl.jcyl.es) and registered to aerial photography with 0.25 m pixels (www.sitcyl.jcyl.es). The multispectral and panchromatic bands were orthorectified separately with root mean square errors (RMSE) of 0.69–0.72 m (multispectral bands) and 0.66–0.81 m (panchromatic band). Images were resampled with cubic convolution to 2.0 m (multispectral bands) and 0.6 m (panchromatic band) for alignment with the regionally appropriate coordinate grid (UTM 30N) and to facilitate integration with rasterized attributes. Atmospheric correction of the multispectral images was performed with the COST model [53] using water bodies as dark objects and the atmosphere-scattered path radiance L_λ^p estimated with a relative spectral scattering DOS model (λ^{-4}) under very clear atmospheric conditions [54].

Table 2. Characteristics of the satellite imagery used in the study.

QuickBird-2 Imagery		
Spatial resolution	Multispectral	2.4 m
	Panchromatic	0.68 m
Bands	Blue	0.45–0.52 μm
	Green	0.52–0.60 μm
	Red	0.63–0.69 μm
	NIR	0.76–0.90 μm
	Pan	0.45–0.90 μm
	Valsaín	*Iruelas*
Date (dd/mm/yyyy)	19/05/2004	05/08/2005
Sun elevation (°)	58.4	72.0

3.3. Image Segmentation

Image segmentation is the partitioning of images into uniform continuous spatial units [55]. Through the application of automated algorithms the criteria for homogeneity can be defined by the user, based on parameters such as tone or spatial pattern. Image objects or segments composed of various pixels provide supplementary features for image analysis, not available in pixel based analysis, such as local statistical relations of digital numbers [37], shape, size or context. That is, once segments are produced, objects (*i.e.*, trees or groups of trees) or spatially constrained summaries of the digital numbers within the segment may be used to provide representative segment-level information [39]. In forest environments, the segments can often be considered as analogous to the manually delineated stands found in forest inventories [56].

Segmentation routines were applied to the QuickBird-2 images using Definiens Cognition Network Technology® [57,58]. In the process of image segmentation the size of resulting objects is determined by the scale parameter and by the landscape characteristics; for instance a given scale value would

produce larger objects in a homogeneous landscape and smaller objects in irregular areas. The scale parameter was 50 in *Iruelas* and 100 in *Valsaín*. Other settings guiding the segmentation routine include color-shape 0.8-0.2 and smoothness-compactness 0.5-0.5. The homogeneity criteria included the visible and NIR bands with similar weight, and an aspect layer derived from the DEM to incorporate topographic information as one of the possible structural driving factors [59] was weighted 0.1.

3.4. Image Texture Metrics

Image texture, defined by Haralick and Bryant [60] as "the pattern of spatial distributions of grey-tone", describes the relationship between elements of surface cover [61] and is one of the most valuable criteria in visual interpretation. The estimation of forest stand parameters is sometimes improved with a combination of spectral and spatial information [62] such as texture. Consequently a host of texture measures have been utilized to predict structural parameters in various environments [13,29,55,63,64] and has shown particular utility in complex structures such as tropical forests for above ground biomass estimation [17,65].

Table 3. Attributes used for modeling. The mean and standard deviation of each of these attributes was *de facto* used in the decision trees.

Predictor Variable	**Description**
Reflectance	
B1 (Blue)	Reflectance band 1
B2 (Green)	Reflectance band 2
B3 (Red)	Reflectance band 3
B4 (NIR)	Reflectance band 4
Textural	
H_S	Homogeneity Small window
Con_S	Contrast Small window
E_S	Entropy Small window
H_M	Homogeneity Medium window
Con_M	Contrast Medium window
E_M	Entropy Medium window
H_L	Homogeneity Large window
Con_L	Contrast Large window
E_L	Entropy Large window
Topographic	
Aspect	Orientation

We applied an approach for texture analysis based on measures derived from the Grey Level Coocurrence Matrix (GLCM) [66,67]. The GLCM is a tabulation of how often different combinations of pixel grey levels occur in an image [68] at a specific distance and orientation (within a particular processing kernel, or analysis window). Texture analysis is a multiscale phenomenon [69] and choosing the right window size to capture meaningful local variance without generalizing unrelated

features [13] is one of its key challenges [70]. For selection of window sizes to calculate the GLCM texture measures we used the semivariogram approach [71,72]. Semivariograms were calculated for image subsets over five experimental structural plots in *Valsaín* [73] and ten structurally different areas in *Iruelas*, identified with a combined approach based on inventory data and visual interpretation to cover all distinctive structural conditions. The range in the variogram indicates the distance beyond which pixel values are no longer correlated [71] and is an indication of the elements forming the texture present within the scene. The range is frequently associated with the most dominant elements in the scene, be it single tree crowns in open forests, or the canopy of groups of trees in close environments. Once the variograms were calculated, the range values were manually identified at the lag distance, where the variograms first flattened, corresponding with window sizes on the QuickBird-2 panchromatic band of 7 × 7, 9 × 9, and 13 × 13 pixels in *Valsaín* and 7 × 7, 13 × 13, and 23 × 23 pixels in *Iruelas*. We considered three GLCM texture variables, that is, *Homogeneity*, *Contrast*, and *Entropy* for each size of window (Small, Medium, and Large) (Table 3) based on their high values of correlation with structural parameters observed and pre-analysis investigations (results not shown).

3.5. Decision Tree

One option to identify relations between variables in multivariate data sets resulting from object analysis is the use of decision tree data analysis [37] also known as Classification and Regression Trees (CART). Regression trees identify relationships between a single continuous response (dependent variable) and multiple, continuous and/or discrete, explanatory (independent) variables, through a binary recursive partitioning process, where the data are split repeatedly into increasingly homogeneous groups (nodes), using combinations of variables (rules) that best distinguish the variation of the response variable. Tree models do not make assumptions regarding the distribution of the input data [74,75]; plus, they are able to capture non linear relationships between variables and are robust to errors in the input and results. Tree modeling is a nonparametric method which basic theory is reported in Breiman *et al.* [76].

CART approaches have frequently been used in the environmental remote sensing community for classification and mapping [77–79] for modeling [80–82] and for forest characterization [83]. In the estimation of forest structural parameters with HSR satellite imagery, decision trees have been applied in diverse environments: Chubey *et al.* [37] used CART for analysis of percent species composition, crown closure, stand height, and age with IKONOS imagery based on analysis of objects in Alberta, Canada, obtaining the best estimations for species composition and crown closure. Goetz *et al.* [84] used IKONOS and shadow analysis to model and derive classified maps of canopy cover, with 97.3% overall accuracy, in Maryland, USA. Mora *et al.* [40] estimated mean height of forest stands in boreal coniferous forests in Yukon, Canada, obtaining a prediction accuracy of 53% and an RMSE of 2.84 m on stand height. All of the abovementioned approaches suggest local models for estimation of forest structural parameters as an alternative tool for alleviation of often costly and time consuming field inventories.

3.6. Applied Decision Tree

For development of decision tree models each segment was characterized with the mean and standard deviation of the reflectance and texture variables described above (Table 3), and the mean

values of the kriged forest structural parameters (QMD, BA, N) and topographic orientation. These sets of data were input for the CART analysis in Matlab®.

Samples were randomly split into calibration (two thirds) and validation (one third) sets. The representativeness of the subsamples was tested with a Multi Response Permutation Procedure (MRPP) [85,86]. This non-parametric method tests the hypothesis of no difference between two or more data sets for a range of parameters (*i.e.*, the metrics used as inputs to the regression tree). To fit the model a cross validation process with ten iterations was performed; to avoid over-fitting we considered the establishment of a minimum number of cases in terminal nodes and pruning with the 1 SE rule [76].

4. Results

4.1. Stand-Like Areas Produced by Segmentation of the QuickBird-2 Imagery

Objects smaller than 0.5 ha produced in the process of segmentation were eliminated. Furthermore, screening outliers of reflectance and texture variables (*i.e.*, segments which values were three or more standard deviations from the mean) enabled identification of objects that did not appear representative of known local forest conditions, typically corresponding with shepherding areas with buildings present in *Valsaín* and objects dominated by bare soil in *Iruelas*. Thirty nine such unusual objects were removed as outliers for subsequent analysis. Finally the number of objects preserved for modeling was 490, with an average area of 5.3 ha. Table 4 lists the statistical descriptors of the structural attributes (QMD, BA, N) and topographic parameter (aspect) at the stand-like level. Figure 3 illustrates the distribution of the structural parameters.

Table 4. Statistical descriptors of structural (QMD, BA, N) and topographic (aspect) parameters of the stand-like objects obtained with the segmentation process and after removal of outliers. To fully capture the ecological meaning of the stand orientation and to avoid operational ambiguities we computed aspect values to be expressed as a non-polar complex number using the notation of Euler: Aspect = $\exp(-i \times (\theta - \Pi/2))$.

	QMD(m)	BA(m^2/ha)	N(n/ha)	Aspect (θ°)
Mean	0.5715	26.5344	323.2064	168.5636
Standard Error	0.0138	0.5044	6.4277	4.3050
Median	0.3918	26.5148	306.461	155.2855
Standard Deviation	0.3062	11.1671	142.2839	95.2968
Kurtosis	−0.7460	−0.6941	0.1987	−1.2352
Skewness	0.7943	0.2266	0.6035	0.1926
Range	1.2407	53.8552	805.0587	337.2344
Minimum	0.2148	5.8128	39.1273	10.1746
Maximum	1.4555	59.6681	844.186	347.4090

Figure 3. Distribution of the structural parameters (QMD, BA, N) in the stand-like polygons produced with the segmentation of the satellite images. Note that QMD graph bins are not all equal.

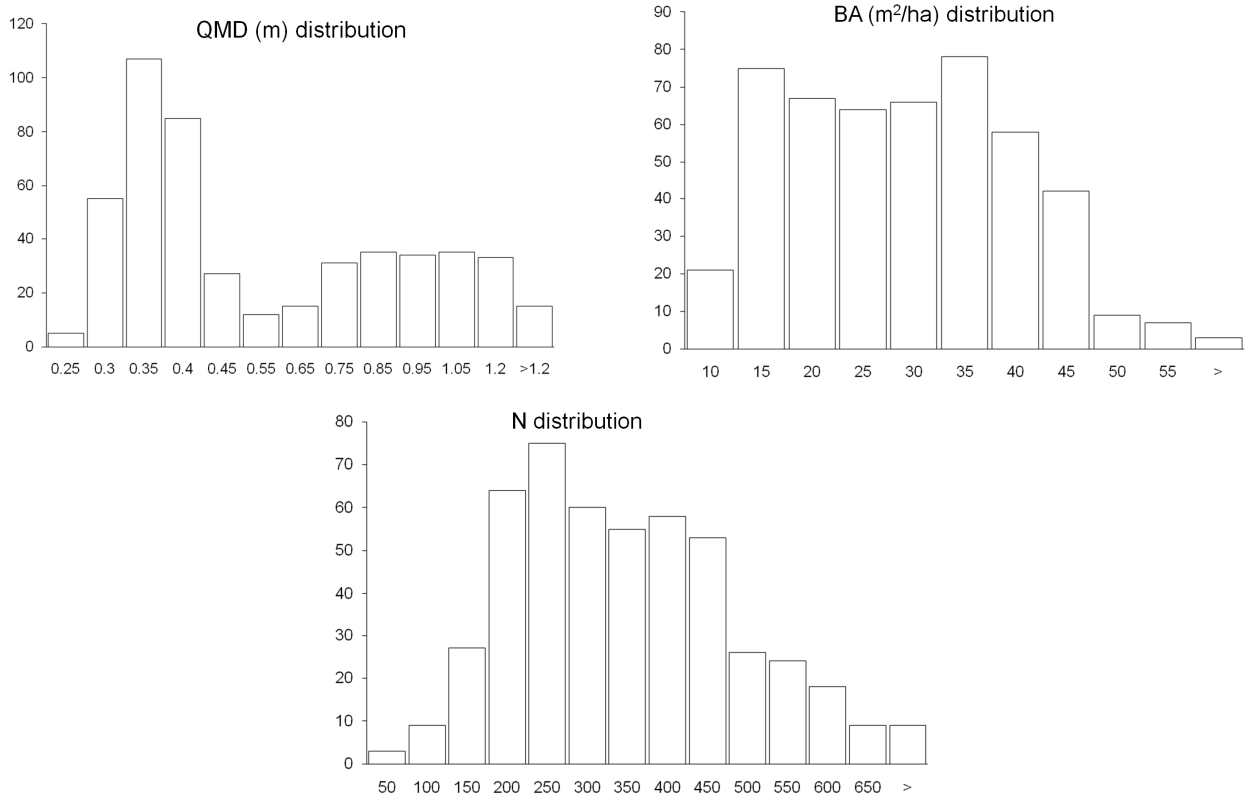

4.2. Regression Trees

Information regarding the calibration and validation subsamples is presented in Table 5. The MRPP test, performed including all stand level predictors, confirmed there were no significant differences between the calibration and validation datasets (p-value 0.77).

Table 5. Number of samples used for calibration and validation of the CART models.

Samples	Stand-Like Segments
Total	490
Calibration	327
Validation	163

Fitting all regression tree models was statistically significant (p-value < 0.001) and with high values of correlation (Table 6) between structural parameters and image predictors. To assess the performance of the models we applied them to the independent set of validation data, analyzing values of the Root Mean Square Error (RMSE) and correlation coefficient (R^2) (Table 6) and evaluating discrepancies between values measured on the field and values predicted by the regression tree models with the help of graphic tools (Figures 4 and 5).

Applied to the validation sample the models show varying strength of the relation between the structural parameters and the image variables used as predictors. The QMD model correlation value is the highest, followed by the BA model and with the N model ranking last (Table 6). The RMSE

values, a means to measure the precision of the models, are moderate for QMD and BA, and relatively higher for N when a prediction of the exact number of trees is expected (Table 6). As practical decisions in forest management are often based on classes of attributes rather than exact values of structural parameters, we evaluated the performance of the CART model to classify values of N. The measured number of trees per unit area (N) was classified into density categories ranging from open (N < 150) to closed (N > 500) categories. The CART model classified 70% of the stand-like segments in the correct group, with all other segments classified in an adjacent class. The average relative error of the models was also evaluated as the percentage of RMSE respect to the average measured parameter (Table 6).

Table 6. Fitting and performance results of the regression tree models for QMD, BA, and N.

Structural Parameter	Validation		Fitting		
	RMSE	% Average Error	R^2	Rho	*p*-value
QMD	0.13	17	0.80	0.89	1.81 e-59
BA	5.79	22	0.70	0.85	7.08 e-47
N	98.86	31	0.46	0.71	1.80 e-26

Scatter plots in Figure 4 illustrate the relation of observed values of QMD (a), BA (b) and N (c) *versus* the corresponding estimated values of the validation subsample (n = 163). The QMD model performs with very good accuracy for the smaller diameters, with points close to the 1:1 line, and more randomly spread to both sides for larger diameters. The BA model depicts a similar but less accurate pattern, while the N model shows increasing disagreement of observed to modeled values at the more dense stands. Noteworthy is a tendency of underestimation for parameters at high values (QMD ≥ 1.2, BA ≥ 50, and N ≥ 600), likely as an expression of the well known saturation of optical sensors at increasingly high biophysical parameter values [34,87]. This kind of error is important to note with reference to volume and biomass estimation, since larger trees contribute more to these estimates [88], but it is of minor importance in this particular area where few stands are over the thresholds mentioned above (Figure 3; Table 4).

Figure 4. Plot of the observed structural parameters QMD (**a**), BA (**b**), and N (**c**), *versus* estimated values for the validation subsample (n = 163).

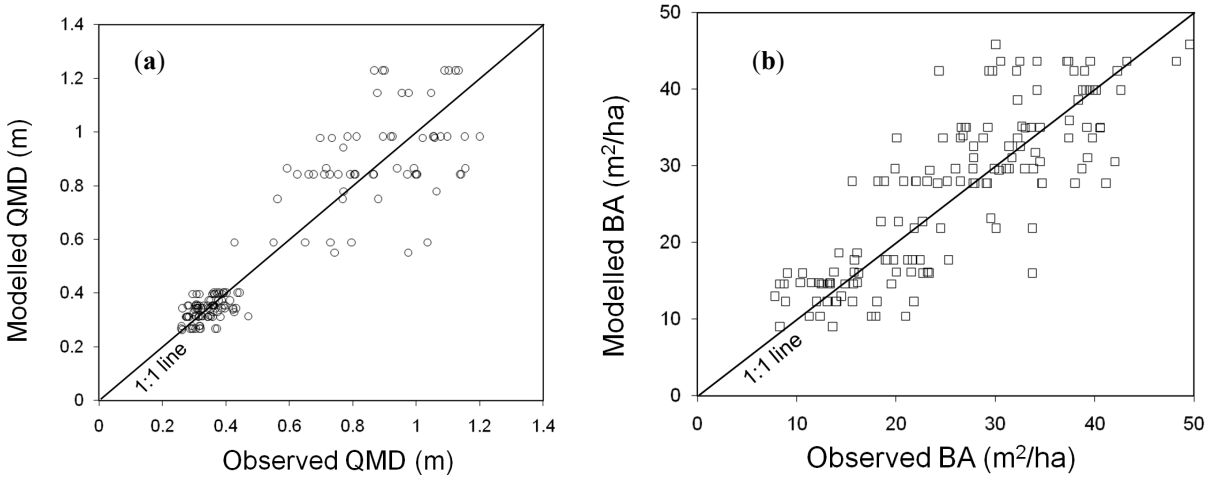

Figure 4. *Cont.*

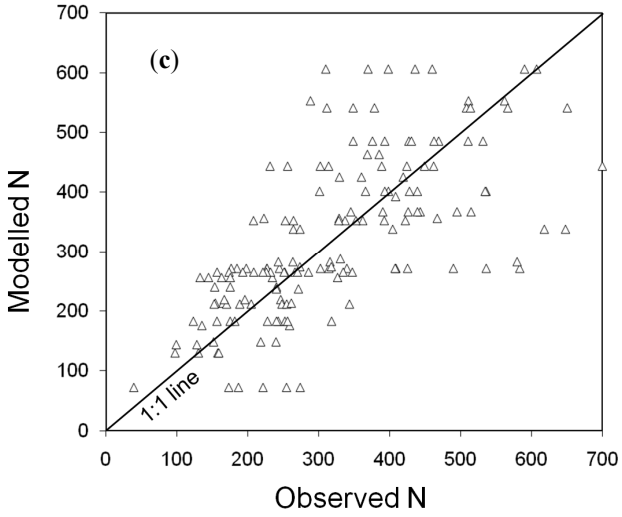

A closer look at the residuals confirms the relative precision of the QMD model (Figure 5(a)); an assessment of relative errors revealed that the relative error committed is below 20% in 76% of the validation sample (n = 123). A comparison of 5 cm diametric classes between the estimated and observed data indicated an agreement in 53% of the stand-like segments, with 19% falling in the adjacent class. Furthermore, the random distribution of residuals in the most frequent classes (0.30–0.40) leads to an almost complete compensation of the average error. This optimistic result should be carefully considered, as averaged values over areas of different sizes could lead to miscalculations. The residuals in the BA model look randomly distributed (Figure 5(b)), but there is a higher number of underestimates (57% of the validation sample) and in these cases the absolute value of residuals is higher. In the N model 55% of the validation segments are underestimated; a tendency to underestimate lower values and overestimate higher densities is observed.

Figure 5. Plot of the observed QMD, BA, and N *versus* the residuals of the models. (**a**): QMD, (**b**): BA, (**c**): N.

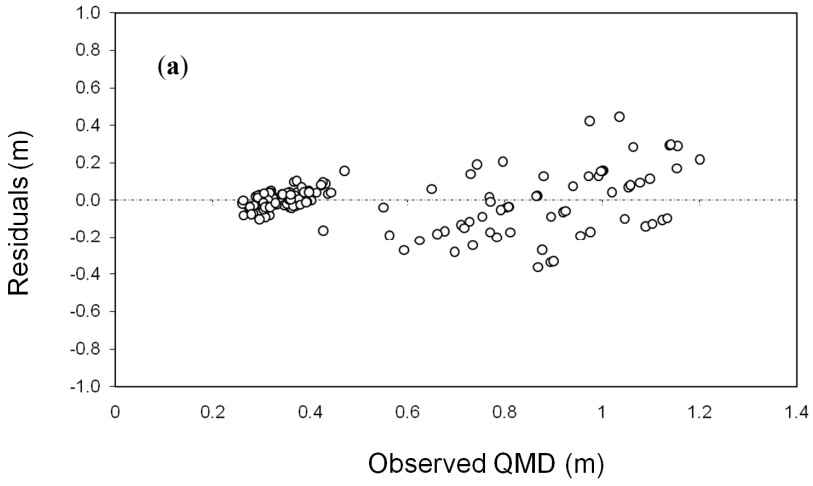

Figure 5. *Cont.*

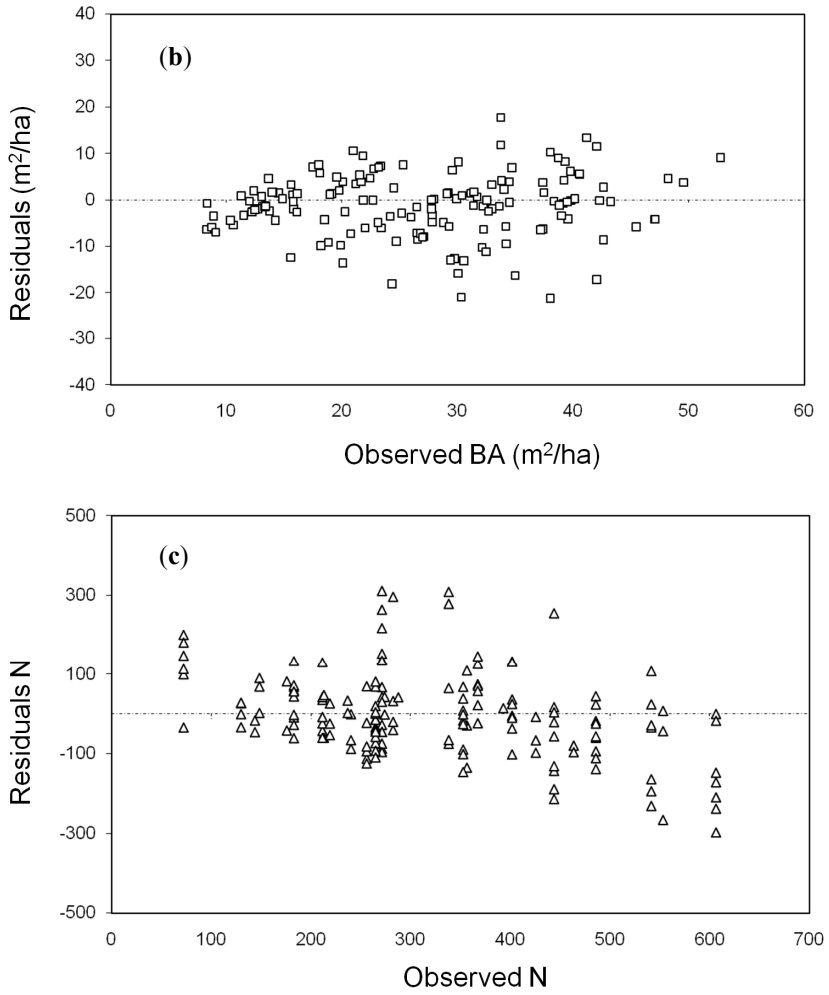

To reduce over-fitting and to make the models practical and operationally viable we established a minimum number of cases in terminal nodes (n = 80). Furthermore, examining the terminal nodes average values and the improvement of intra-group variance they represent from father nodes (*i.e.*, decreased variance) appropriate pruning levels were determined. With these premises the number of terminal nodes obtained was between seven (for the QMD and BA models) and eight (for the N model) (Figure 6; Table 7).

The most relevant predicting variables determining decisions in the regression tree models are shown in Table 7. Noteworthy is the primacy of stdev B1 (standard deviation of blue reflectance) which enters all models in first place. All other reflectance bands (green, red and near-infrared) did also determine some branch rules (Figure 6). Among textural variables, contrast and entropy of various window sizes were the more relevant; homogeneity was not included in decision rules. A total of five or six variables were included in each of the models.

Figure 6. Example of a regression tree model of QMD. Hollow boxes represent branch rules; elements fulfilling the rule go to the left, the rest go to the right. Values of terminal nodes average QMD of elements in the group.

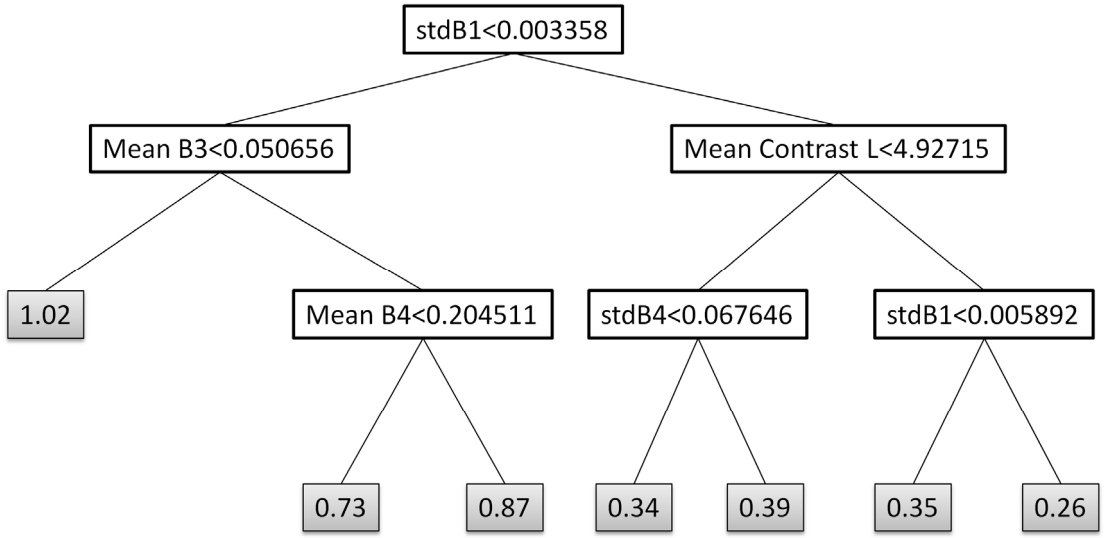

Table 7. Relevant predictors in regression trees of QMD, BA and N and number of terminal nodes.

Structural Parameter	Relevant Predictors	Terminal Nodes
QMD	*Stdev B1* *Mean B3* *Mean Contrast Larger window* *Mean B4* *Standard deviation B4*	7
BA	*Stdev B1* *Mean B3* *Mean B1* *Standard deviation B2* *Mean Entropy Small window*	7
N	*Stdev B1* *Mean B1* *Standard deviation B4* *Mean Entropy Medium window* *Mean B2* *Mean B3*	8

5. Discussion

Structural parameters such as quadratic mean diameter, basal area, and number of trees per unit area of Mediterranean pines in Central Spain have been modeled with regression trees and with HSR reflectance and texture metrics from QuickBird-2 imagery as model inputs. Results, although limited by uncertainties in the reference data and processing techniques, show reasonable accuracy ($R^2 = 0.8$) and precision (estimation relative error ~17%) for the QMD model and robust models ($R > 0.7$) for BA and N but with higher estimation relative error (22–31%).

Management plans were initiated in Spanish forests more than a hundred years ago [89]. Albeit the early start, only 19% of the treed forest area in Spain is currently governed by a management plan under formal implementation [90]. Often noted as a primary reason for this unfavorable proportion, is the high cost of field inventories, limiting surveys to forests with potential to produce economic revenue. However, with the increasing concern over environmental issues, current forest inventories are aimed at informing a variety of long-term objectives including biodiversity, carbon accounting, habitat protection and sustainable timber production [91]. Remote sensing can contribute to the ability to produce timely, cost efficient inventory estimates via image segmentation for stand delineation [45] and statistical modeling for assessment of attributes with acceptable precision [5]. HSR satellite sensors emerged a few years ago as promising data sources for forest inventory [6,92] providing consistent and frequent imagery. Our study demonstrates that in Mediterranean pines of Spain QuickBird-2 imagery and CART modeling would be useful and affordable for assisting in the assessment of forest areas with a variety of objectives (e.g., recreation, carbon storage), though caution is required to deal with inherent modeling uncertainties. Although remote sensing is not expected to replace completely field measurement any time in the near future [5] it would facilitate planning and management with realistic goals.

Among the strengths of HSR imagery is the high geometric fidelity [93] and the possibility of identification of individual elements such as trees or groups of trees. The unique capabilities of the QuickBird-2 instrument are exploited here by including texture metrics in the modeling, as image texture is influenced by biophysical parameters like crown diameter, distance between trees, tree positioning, LAI, and tree height. The historic limited use of texture parameters is often indicated as related to a paucity of appropriate software tools [94] and is being progressively overcome. Alternately, for monitoring programs with various dates of imagery and more than one scene, off-nadir view angles and differing solar and atmospheric conditions should be considered [20] as they may pose analysis difficulties.

Heterogeneous environments typically require a dense network of sample plots for an adequate assessment of varying conditions [95]; likewise, the capacity of a grid of inventory plots to capture the diversity of Mediterranean forests could be argued. With the complete coverage offered by remotely sensed data, selective sampling may become unnecessary, for instance if imputation techniques are applied. Furthermore, in applications where sampling is needed, segmentation of HSR images helps the design of sampling units by automatically and consistently defining homogeneous areas [96], otherwise delineated with human expert and costly effort. If adequately trained, segmentation algorithms have the ability to semi-automatically divide images into structurally homogeneous areas only requiring human revision [25], that can be used as strata to optimize the field sampling design [97] and also allowing the reduction of sample collection needs.

Tree models are easily interpreted and applied, with few statistical requirements imposed that make it an appropriate method of estimation in forest environments. Employing data from managed stands' field inventories in the support of modeling efforts has an intrinsic limitation related to the dearth of measurements of small trees; this circumstance is possibly related to a bias of the data considered as truth, and could partly excuse the underestimating trend of our models. All sources of uncertainty should be thoroughly considered for aiding the interpretation of modeling results. Our calibration dataset consisting of 327 stands is relatively large (66% of the sample) as the accuracy of decision tree

models tends to increase with increasing calibration sample size [70]. Mora *et al.* [40] in Yukon (Canada) demonstrated that a smaller calibration dataset (30% of the sample) could perform adequately if there were difficulties to obtain reference information, making this method an even more appealing tool for inventory. With a simple structure, that is, low number of rules and final nodes, CART constitute a practical and parsimonious tool for classification of stands for management or planning. The acquisition of periodic HSR coverage of the whole territory by the PNT poses an unprecedented opportunity to use remote sensing for assessment of the structure of Spanish forests that managers should strongly consider.

6. Conclusions

High spatial resolution (HSR) satellite imagery, such as QuickBird-2, has information content enabling the modeling of structural parameters for the pine forests of Central Spain. In this research the quadratic mean diameter (QMD), basal area (BA), and number of trees per hectare (N) of pines in the Central Range of Spain were modeled at the stand level with classification and regression trees (CART). Models were produced with average estimation errors suitable for planning purposes: predictions of QMD had an average error of 17% and BA an average error of 22%, while N was correctly classified in 70% of the cases. Although some refinement of the techniques applied here is possible to support operational activities, this study has demonstrated that following the selection of appropriate statistical tools combined with the periodic acquisition of HSR imagery by the Spanish Plan Nacional de Teledetección (PNT) could be of great value to the forest community as a low cost option to support planning activities. Additional stakeholders could also be accommodated and supplied with wide-area estimates of forest structural attributes following the methods suggested in this research. The capacity to revise the estimates with new plot data in subsequent years and to incorporate depletions using change detection procedures also points to additional utility and value that can be created from the national PNT image collections.

Acknowledgments

This work was done under the project “Estructura, dinámica y selvicultura para la conservación y el uso sostenible de los bosques en el Sistema Central” (VA-096-A05) with funding from Consejería de Educación, Junta de Castilla y León, Plan Regional I+D+I. Field data was provided by Consejería de Medio Ambiente y Ordenación Territorial de Castilla y León. Brice Mora and Wolfgang Schwanghart are thanked for their help with data analysis.

References

1. European Forest Institute, Mediterranean Regional Office. *A Mediterranean Forest Research Agenda-MFRA 2010–2020*; EFIMED: Barcelona, Spain, 2009.
2. Chirici, G.; Barbati, A.; Corona, P.; Marchetti, M.; Travaglini, D.; Maselli, F.; Bertini, R. Non-parametric and parametric methods using satellite images for estimating growing stock volume in alpine and Mediterranean forest ecosystems. *Remote Sens. Environ.* **2008**, *112*, 2686-2700.

3. Bravo, F.; Montero, G. High-grading effects on Scots pine volume and basal area in pure stands in northern Spain. *Ann. For. Sci.* **2003**, *60*, 11-18.
4. Bellassen, V.; Maire, G.; Dhote, J.F.; Ciais, P.; Viovy, N. Modelling forest management within a global vegetation model-Part 2: Model validation from a tree to a continental scale. *Ecol. Model.* **2011**, *222*, 57-75.
5. McRoberts, R.E.; Tomppo, E.O. Remote sensing support for national forests inventories. *Remote Sens. Environ.* **2007**, *110*, 412-419.
6. Falkowski, M.J.; Wulder, M.A.; White, J.C.; Gillis, M.D. Supporting large-area, sample-based forest inventories with very high spatial resolution satellite imagery. *Prog. Phys. Geog.* **2009**, *33*, 403-423.
7. Wulder, M.A. Optical remote sensing techniques for the assessment of forest inventory and biophysical parameters. *Prog. Phys. Geog.* **1998**, *22*, 449-476.
8. Wulder, M.A.; White, J.C.; Han, T.; Coops, N.C.; Cardille J.A.; Holland, T.; Grills, D. Monitoring Canada forests. Part 2: National forest fragmentation and pattern. *Can. J. Remote Sens.* **2008**, *34*, 563-584.
9. Wulder, M.A.; Hall, R.J.; Coops, N.C.; Franklin, S.E. High spatial resolution remotely sensed data for ecosystem characterization. *Bioscience* **2004**, *54*, 511-521.
10. Andersson, K.; Evans, T.P.; Richards, K.R. National forest carbon inventories: Policy needs and assessment capacity. *Climatic Change* **2009**, *93*, 69-101.
11. Cohen, W.; Goward, S. Landsat's role in ecological applications of remote sensing. *BioScience* **2004**, *54*, 535-545.
12. Wulder, M.A.; White, J.C.; Goward, S.N.; Masek, J.G.; Irons, J.R.; Herold, M.; Cohen, W.B.; Loveland, T.R.; Woodcock, C.E. Landsat continuity: Issues and opportunities for land cover monitoring. *Remote Sens. Environ.* **2008**, *112*, 955-969.
13. Kayitakire, F.; Hamel, C.; Defourny, P. Retrieving forest structure variables based on image texture analysis and IKONOS-2 imagery. *Remote Sens. Environ.* **2006**, *102*, 390-401.
14. Colombo, R.; Bellingeri, D.; Fasolini, D.; Marino, C.M. Retrieval of leaf area index in different vegetation types using high resolution satellite data. *Remote Sens. Environ.* **2003**, *83*, 120-131.
15. Ouma, Y.O.; Ngigi, T.G.; Tateishi, R. On the optimization and selection of wavelet texture for feature extraction from high resolution satellite imagery with application towards urban tree delineation. *Int. J. Remote Sens.* **2006**, *27*, 73-104.
16. Song, C.; Dickinson, M.B.; Su, L.; Zhang, S.; Yaussey, D. Estimating average tree crown size using spatial information from IKONOS and QuickBird images: Across-sensor and across-site comparisons. *Remote Sens. Environ.* **2010**, *114*, 1099-1107.
17. Lu, D.; Mausel, P.; Brondizio, E.; Moran, E. Above-Ground Biomass estimation of Successional and Mature Forests Using TM Images in the Amazon Basin. In *Proceedings of Symposium on Geospatial Theory, Processing and Applications*, Otawa, ON, Canada, 9–12 July 2002.
18. Ozdemir, I. Estimating stem volume by tree crown area and tree shadow area extracted from pan-sharpened QuickBird imagery in open Crimean juniper forests. *Int. J. Remote Sens.* **2008**, *29*, 5643-5655.
19. Pu, R.; Landry, S.; Yu, Q. Object-based urban detailed land cover classification with high spatial resolution IKONOS imagery. *Int. J. Remote Sens.* **2011**, *32*, 3285-3308.

20. Wulder, M.A.; Ortlepp, S.M.; White, J.C.; Coops, N.C. Impact of sun-surface sensor geometry upon multitemporal high spatial resolution satellite imagery. *Can. J. Remote Sens.* **2008**, *34*, 455-461.
21. Lefsky, M.A.; Cohen, W.B.; Acker, S.A.; Parker, G.G.; Spies, T.A.; Harding, D. Lidar remote sensing of the canopy structure and biophysical properties of Douglas-fir Western Hemlock forests. *Remote Sens. Environ.* **1999**, *70*, 339-361.
22. Lim, K.; Treitz, P.; Baldwin, K.; Morrison I.; Green, J. Lidar remote sensing of biophysical properties of tolerant northern hardwood forests. *Can. J. Remote Sens.* **2003**, *29*, 658-678.
23. Riaño, D.; Chuvieco, E.; Condés, S.; González-Matesanz, J.; Ustin, S.L. Generation of crown bulk density for *Pinus sylvestris* L. from lidar. *Remote Sens. Environ.* **2004**, *92*, 345-352.
24. Zhao, K.; Popescu, S.; Meng, X.; Pang, Y.; Agca, M. Characterizing forest canopy structure with lidar composite metrics and machine learning. *Remote Sens. Environ.* **2011**, *115*, 1978-1996.
25. Wulder, M.A.; White, J.C.; Hay, G.J.; Castilla, G. Towards automated segmentation of forest inventory polygons on high spatial resolution satellite imagery. *Forest. Chron.* **2008**, *84*, 221-230.
26. Gougeon, F.A.; Leckie, D.G. The individual tree crown approach applied to IKONOS images of a coniferous plantation area. *Photogram. Eng. Remote Sensing* **2006**, *72*, 1287-1297.
27. Hirata, Y. Estimation of stand attributes in *Cryptomeria japonica* and *Chamaecyparis obtusa* stands using QuickBird panchromatic data. *J. Forest Res.* **2008**, *13*, 147-154.
28. Leboeuf, A.; Beaudoin, A.; Fournier, R.A.; Guindon, L.; Luther, J.E.; Lambert, M.C. A shadow fraction method for mapping biomass of northern boreal black spruce forests using QuickBird imagery. *Remote Sens. Environ.* **2007**, *110*, 488-500.
29. Franklin, S.E.; Wulder, M.A.; Gerylo, G.R. Texture analysis of IKONOS panchromatic data for Douglas-fir forest age class separability in British Columbia. *Int. J. Remote Sens.* **2001**, *22*, 2627-2632.
30. Ozdemir, I.; Norton, D.A.; Ozkan, U.Y.; Mert, A.; Senturk, O. Estimation of tree size diversity using object oriented texture analysis and ASTER imagery. *Sensors* **2008**, *8*, 4709-4724.
31. Song, C. Estimating tree crown size with spatial information of high resolution optical remotely sensed imagery. *Int. J. Remote Sens.* **2007**, *28*, 3305-3322.
32. Feng, Y.; Li, Z.; Tokola, T. Estimation of stand mean crown diameter from high-spatial-resolution imagery based on a geostatistical method. *Int. J. Remote Sens.* **2010**, *31*, 363-378.
33. Merino de Miguel, S.; Solana Gutiérrez, J.; González Alonso, F. Análisis de la estructura espacial de las masas de *Pinus pinaster* Aiton de la Comunidad de Madrid mediante imágenes de alta resolución espacial. *Forest Syst.* **2010**, *19*, 18-35.
34. Duncanson, L.I.; Niemann, K.O.; Wulder, M.A. Integration of GLAS and Landsat TM data for aboveground biomass estimation. *Can. J. Remote Sens.* **2010**, *36*, 129-141.
35. Greenberg, J.A.; Dobrowsky, S.Z.; Ustin, S.L. Shadow allometry: Estimating tree structural parameters using hyperspatial image analysis. *Remote Sens. Environ.* **2005**, *97*, 15-25.
36. Hyde, P.; Dubayah, R.; Walker, W.; Blair, B.; Hofton, M.; Hunsaker, C. Mapping forest structure for wildlife habitat analysis using multi-sensor (LiDAR, SAR/InSAR, ETM+, Quickbird) synergy. *Remote Sens. Environ.* **2006**, *102*, 63-73.
37. Chubey, M.S.; Franklin, S.E.; Wulder, M.A. Object-based analysis of IKONOS-2 imagery for extraction of forest inventory parameters. *Photogramm. Eng. Remote Sensing* **2006**, *72*, 383-394.

38. Proisy, Ch.; Couteron, P.; Fromard, F. Predicting and mapping mangrove biomass from canopy grain analysis using Fourier-based textural ordination of IKONOS images. *Remote Sens. Environ.* **2007**, *109*, 379-392.
39. Palace, M.; Keller, M.; Asner, G.P.; Hagen, S.; Braswell, B. Amazon forest structure from IKONOS satellite data and the automated characterization of forest canopy properties. *Biotropica* **2008**, *40*, 141-150.
40. Mora, B.; Wulder, M.A.; White, J.C. Segment-constrained regression tree estimation of forest stand height from very high spatial resolution panchromatic imagery over a boreal environment. *Remote Sens. Environ.* **2010**, *114*, 2474-2484.
41. Arozarena A. El Plan Nacional de Observación del territorio en España como sistema básico de información Medio Ambiental. In *Congreso Nacional del Medio Ambiente*, Cumbre del Desarrollo Sostenible, Madrid, Spain, 1–5 December 2008.
42. Villa, G.; Arozarena, A.; Peces, J.J.; Domenech, E. Plan nacional de teledetección: estado actual y perspectivas futuras. In *Proceedings of Teledetección: agua y desarrollo sostenible. XIII Congreso de la Asociación Española de Teledetección*, Calatayud, Spain, 23–26 September 2009; pp. 521-524.
43. IGN. *Plan Nacional de Teledetección (PNT)*; Versión 2.3; Ministerio de Fomento, Gobierno de España: Madrid, Spain, 2009.
44. Vázquez de la Cueva, A. Structural attributes of three forest types in central Spain and Landsat ETM+ information evaluated with redundancy analysis. *Int. J. Remote Sens.* **2008**, *29*, 5657-5676.
45. Pascual, C.; García Abril, A.; García Montero, L.G.; Martín Fernández, S.; Cohen, W.B. Object-based semi-automatic approach for forest structure characterization using lidar data in heterogeneous *Pinus sylvestris* stands. *Forest Ecol. Manag.* **2008**, *255*, 3677-3685.
46. Montes, F.; Sánchez, M.; Río, M.; Cañellas, I. Using historic management records to characterize the effects of management on the structural diversity of forests. *Forest Ecol. Manag.* **2004**, *207*, 279-293.
47. Bravo, F.; Río, M.; Pando, V.; San Martín, R.; Montero, G.; Ordoñez, C.; Cañellas, I. El diseño de las parcelas del inventario forestal nacional y la estimación de variables dasómetricas. In *El Inventario Forestal Nacional, Elemento Clave para la Gestión Forestal Sostenible*; Bravo, F., Rio, M., Peso, C., Eds.; Fundación General de la Universidad de Valladolid: Valladolid, Spain, 2002; pp. 19-35.
48. Curtis, R.O.; Marshall, D.D. Why quadratic mean diameter? *West. J. Appl. For*. **2000**, *15*, 137-139.
49. Chica-Olmo, M. La geoestadística como herramienta de análisis en la gestión forestal. *Cuad. Soc. Esp. Cienc. For*. **2005**, *19*, 47-55.
50. Curran, P.J.; Atkinson, P.M. Geostatistics and remote sensing. *Prog. Phys. Geog.* **1998**, *22*, 61-78.
51. Clark, I. *Practical Geostatistics*; Geostokos Limited: Scotland, UK, 2001. Available online: http://w3eos.whoi.edu/12.747/resources/pract_geostat/pg1979_latex.pdf (accessed on 17 May 2011).
52. DigitalGlobe. *QuickBird Imagery Products FAQ*; Houston, TX, USA, 2005. Available online: http://www.satimagingcorp.com/satellite-sensors/quickbird_imagery_products.pdf (accessed on 17 October 2011).

53. Chavez, P.S. Image-based atmospheric corrections—Revisited and improved. *Photogramm. Eng. Remote Sensing* **1996**, *62*, 1025-1036.
54. Chavez, P. An improved dark object subtraction technique for atmospheric scattering correction of multispectral data. *Remote Sens. Environ.* **1988**, *24*, 459-479.
55. Devereux, B.J.; Amable, G.S.; Costa Posada, C. An efficient image segmentation algorithm for landscape analysis. *Int. J. Appl. Earth Obs. Geoinf.* **2004**, *6*, 47-61.
56. Hay, G.J.; Castilla, G.; Wulder, M.A.; Ruiz, J.R. An automated object-based approach for the multiscale image segmentation of forest scenes. *Int. J. Appl. Earth Obs. Geoinf.* **2005**, *7*, 339-359.
57. Baatz, M.; Schäpe, M. Multiresolution segmentation—An optimization approach for high quality multi-scale image segmentation. In *Angewandte Geographische Informations-Verarbeitung XII.*; Strobl, J., Blaschke, T., Griesebner, G., Eds.; Wichmann Verlag: Karlsruhe, Germany, 2000; pp. 12–23.
58. Definiens. *Definiens Professional 5 User Guide*; Definiens: Munich, Germany, 2006.
59. Salvador, R.; Pons, X. On the applicability of Landsat TM images to Mediterranean forest inventories. *Forest Ecol. Manag.* **1998**, *104*, 193-208.
60. Haralick, R.M.; Bryant, W.F. *Documentation of Procedures for Textural/Spatial Pattern Recognition Techniques*; Technical Report 278-1; Remote Sensing Laboratory, University of Kansas: Lawrence, KS, USA, 1976.
61. Wulder, M.A.; LeDrew, E.F.; Franklin, S.E.; Lavigne, M.B. Aerial texture information in the estimation of northern deciduous and mixed wood forest leaf area index (LAI). *Remote Sens. Environ.* **1998**, *64*, 64-76
62. Lu, D. The potential and challenge of remote sensing-based biomass estimation. *Int. J. Remote Sens.* **2006**, *27*, 1297-1328.
63. Franklin, S.E.; Hall, R.J.; Moskal, L.M.; Maudie, A.J.; Lavigne M.B. Incorporating texture into classification of forest species composition from airborne multispectral images. *Int. J. Remote Sens.* **2000**, *21*, 61-79.
64. Couteron, P.; Pelissier, R.; Nicolini, E.A.; Paget, D. Predicting tropical forest stand structure parameters from Fourier transform of very high-resolution remotely sensed canopy images. *J. App. Ecol.* **2005**, *42*, 1121-1128.
65. Lu, D.; Batistella, M. Exploring TM image texture and its relationships with biomass estimation in Rondonia, Brazilian Amazon. *Acta Amazonica* **2005**, *35*, 249-257.
66. Haralick, R.M.; Shanmugan, K.; Dinstein, I. Texture features for image classification. *IEEE T. Syst. Man Cyb.* **1973**, *3*, 610-621.
67. Caridade, C.M.R.; Marca, A.R.S.; Mendonca, T. The use of texture for image classification of black & white air photographs. *Int. J. Remote Sens.* **2008**, *29*, 593-607
68. Hall-Beyer, M. *GLCM Tutorial Home Page*; 2007. Available online: http://www.fp.ucalgary.ca/mhallbey/tutorial.htm (accessed on 13 October 2011).
69. Ahearn, S.C. Combining Laplacian images of different spatial frequencies (scales): Implications for remote sensing analysis. *IEEE Trans. Geosci. Remote Sens.* **1988**, *26*, 826-831.
70. Ferro, C.; Warner, T. Scale and texture in digital image classification. *Photogramm. Eng. Remote Sensing* **2002**, *68*, 51-63.

71. Johansen, K.; Coops, N.C.; Gergel, S.E.; Stange, Y. Application of high spatial resolution satellite imagery for riparian and forest ecosystem classification. *Remote Sens. Environ.* **2007**, *110*, 29-44.
72. Nijland, W.; Addink, E.A.; de Jong, S.M.; Van der Meer, F.D. Optimizing spatial image support for quantitative mapping of natural vegetation. *Remote Sens. Environ.* **2009**, *113*, 771-780.
73. Montes, F.; Rubio, A.; Barbeito, I.; Cañellas, I. Characterization of the spatial structure of the canopy in *Pinus sylvestris* L. stands in Central Spain from hemispherical photographs. *Forest Ecol. Manag.* **2008**, *255*, 580-590.
74. Pal, M.; Mather, P.M. An assessment of the effectiveness of decision tree methods for land cover classification. *Remote Sens. Environ.* **2003**, *86*, 554-565.
75. Baccini, A.; Laporte, N.; Goetz, S.J.; Sun, M.; Dong, H. A first map of tropical Africa's above-ground biomass derived from satellite imagery. *Environ. Res. Let*. **2008**, *3*, 045011
76. Breiman, L.; Friedman, J.H.; Olshen, R.A.; Stone, C.J. *Classification and Regression Trees*; Chapman and Hall/CRC: Boca Raton, FL, USA, 1984; p. 358.
77. Brown de Colstoun, E.C.; Story, M.H.; Thompson, C.; Commisso, K.; Smith, T.G.; Irons, J.R. National Park vegetation mapping using multitemporal Landsat 7 data and a decision tree classifier. *Remote Sens. Environ*. **2003**, *85*, 316-327.
78. Mcdermid, G.J.; Smith, I.U. Mapping the distribution of whitebark pine (*Pinus albicaulis*) in Waterton Lakes National Park using logistic regression and classification tree analysis. *Can. J. Remote Sens.* **2008**, *34*, 356-366.
79. Ke, Y.; Quackenbush, L.J.; Im, J. Synergistic use of QuickBird multispectral imagery and LIDAR data for object-based forest species classification. *Remote Sens. Environ.* **2010**, *114*, 1141-1154.
80. Andrew, M.E.; Ustin, S.L. Habitat Suitability Modeling of an invasive plant with advanced remote sensing data. *Divers. Distrib.* **2009**, *15*, 627-640.
81. Im, J.; Jensen, J.R. A change detection model based on neighborhood correlation image analysis and decision tree classification. *Remote Sens. Environ.* **2005**, *99*, 326-340.
82. Lozano, F.J.; Suárez-Seoane, S.; Kelly, M.; Luis, E. A multi-scale approach for modeling fire occurrence probability using satellite data and classification trees: A case study in a mountainous Mediterranean region. *Remote Sens. Environ.* **2008**, *112*, 708-719.
83. Falkowski, M.J.; Evans, J.; Martinuzzi, S.; Gessler. P.E.; Hudak, A.T. Characterizing forest succession with lidar data: an evaluation for the Inland Northwest, USA. *Remote Sens. Environ.* **2009**, *113*, 946-956.
84. Goetz, S.J.; Wright, R.K.; Smith, A.J.; Zinecker, E.; Schaub, E. IKONOS imagery for resource management: tree cover, impervious surfaces, and riparian buffer analyses in the mid-Atlantic region. *Remote Sens. Environ.* **2003**, *88*, 195-208.
85. Biondini, M.E.; Mielke, P.W., Jr.; Berry, K.J. Data-dependent permutation techniques for the analysis of ecological data. *Vegetatio* **1988**, *75*, 161-168.
86. Mielke, P.W., Jr.; Berry, K.J. *Permutation Methods: A Distance Function Approach*; Springer Series in Statistics; Springer: New York, NY, USA, 2001.
87. Foody, G.M.; Cutler, M.E.; McMorrow, J.; Pelz, D.; Tangki, H.; Boyd, D.S.; Douglas, I. Mapping the biomass of Bornean tropical rain forest from remotely sensed data. *Global Ecol. Biogeogr.* **2001**, *10*, 379-387.

88. Wulder, M.A.; Niemann, K.O.; Goodenough, D.G. Error reduction methods for local maximum filtering. *Can. J. Remote Sens*. **2002**, *28*, 667-671.
89. Bernués, D. La gestión forestal sostenible en Aragon. *Foresta* **2008**, *43*, 104-107.
90. MMA. *Anuario de Estadística Forestal 2008*; Ministerio de Medio Ambiente y Medio Rural y Marino: Madrid, Spain, 2008; p. 96.
91. Wulder, M.A.; Kurz, W.A.; Gillis, M. National level forest monitoring and modeling in Canada. *Prog. Phys. Plan.* **2004**, *61*, 365-381.
92. Culvenor, D.S. Extracting individual tree information: A survey of techniques for high spatial resolution imagery. In *Remote Sensing of Forest Environments: Concepts and Case Studies*; Wulder, M.A., Franklin, S.E. Eds.; Kluwer Academic Publishers: Boston, MA, USA, 2003; pp. 255-277.
93. Aguilar, M.A.; Agüera, F.; Aguilar, F.J.; Carvajal, F. Geometric accuracy assessment of the orthorectification process from very high resolution satellite imagery for common agricultural policy purposes. *Int. J. Remote Sens.* **2008**, *29*, 7181-7197.
94. Bruniquel-Pinel, V.; Gastellu-Etchegorry, J.P. Sensitivity of texture of high resolution images of forest to biophysical and acquisition parameters. *Remote Sens. Environ.* **1998**, *65*, 61-85.
95. Maselli, F. Monitoring forest conditions in a protected Mediterranean coastal area by the analysis of multiyear NDVI data. *Remote Sens. Environ.* **2004**, *89*, 423-433.
96. Leckie, D.G.; Gougeon, F.A.; Walsworth, N.; Paradine, D. Stand delineation and composition estimation using semi-automated individual tree crown analysis. *Remote Sens. Environ.* **2003**, *85*, 355-369.
97. Lamonaca, A.; Corona, P.; Barbati, A. Exploring forest structural complexity by multi-scale segmentation of VHR imagery. *Remote Sens. Environ.* **2008**, *112*, 2839-2849.